COMPUTING CONFORMAL MAPS AND MINIMAL SURFACES

John E. Hutchinson

Department of Mathematics

School of Mathematical Sciences

A.N.U.

Abstract We discuss some recent work on numerical generation of conformal maps and minimal surfaces. Much of this work is joint with Gerd Dziuk. Some of the material on unstable minimal surfaces was developed subsequent to the Workshop.

1. CONFORMAL MAPS

1.1 General Considerations

Suppose D and Ω are simply connected bounded domains in R^2 with C^1 boundaries. Let

(1) $$\mathcal{F} = \big\{u = (u_1, u_2) : D \to \Omega \,\big|\, u \in W^{1,2}(D) \cap C^0(\partial D), \quad u|_{\partial D} \text{is a weakly monotone orientation preserving map onto } \partial\Omega\big\}$$

For fixed $p_1, p_2, p_3 \in \partial D$ and $q_1, q_2, q_3 \in \partial\Omega$ having the same orientation, let

(2) $$\mathcal{F}_* = \big\{u \in \mathcal{F} \,\big|\, u(p_i) = q_i \text{ for } i = 1, 2, 3\big\}.$$

It is well known that there is a unique $u \in \mathcal{F}_*$ which is *conformal.*

For $u \in \mathcal{F}$ let $\sigma_1(x)$ and $\sigma_2(x)$ be the signed singular values of the map $Du(x)$. Thus

$$Du(x) = S \circ O$$

where O is a rotation and S is a symmetric map with eigenvalues $\sigma_1(x)$ and $\sigma_2(x)$. The failure of u to be conformal at x is measured by the quantity

(3) $$\big(\sigma_1(x) - \sigma_2(x)\big)^2 = \sigma_1^2 + \sigma_2^2 - 2\sigma_1\sigma_2.$$

If L is the linear map with matrix $\begin{bmatrix} L_{11} & L_{12} \\ L_{21} & L_{22} \end{bmatrix}$, then $|L|^2 = L_{11}^2 + L_{12}^2 + L_{21}^2 + L_{22}^2$ and $\det L = L_{11}L_{22} - L_{21}L_{12}$ are invariant under orthonormal transformations. Using this, we see that the expression in (3) equals

$$\left(\frac{\partial u_1}{\partial x} - \frac{\partial u_2}{\partial y}\right)^2 + \left(\frac{\partial u_1}{\partial y} + \frac{\partial u_2}{\partial x}\right)^2. \tag{4}$$

Note that this expression equals zero iff the Cauchy Riemann equations are satisfied iff u is conformal. Note also that (4) can be written in the form

$$\left|J\frac{\partial u}{\partial x} - \frac{\partial u}{\partial y}\right|^2, \tag{5}$$

where J is rotation by $\pi/2$. We again see this is a natural measure of the failure of u to be conformal.

Finally we observe that any of (3), (4), (5) can be written in the form

$$\left(\left(\frac{\partial u_1}{\partial x}\right)^2 + \left(\frac{\partial u_1}{\partial y}\right)^2 + \left(\frac{\partial u_2}{\partial x}\right)^2 + \left(\frac{\partial u_2}{\partial y}\right)^2\right) - 2\left(\frac{\partial u_1}{\partial x}\frac{\partial u_2}{\partial y} - \frac{\partial u_1}{\partial y}\frac{\partial u_2}{\partial x}\right), \tag{6}$$

where the second term is the signed Jacobian of the map u.

Motivated by all this we define the *conformal energy* of u to be

$$\begin{aligned} E_C(u) &= \frac{1}{2}\int_D \left(\frac{\partial u_1}{\partial x} - \frac{\partial u_2}{\partial y}\right)^2 + \left(\frac{\partial u_1}{\partial y} + \frac{\partial u_2}{\partial x}\right)^2 \\ &= \frac{1}{2}\int_D \left|J\frac{\partial u}{\partial x} - \frac{\partial u}{\partial y}\right|^2 \qquad (7) \\ &= \frac{1}{2}\int_D \left(\left(\frac{\partial u_1}{\partial x}\right)^2 + \left(\frac{\partial u_1}{\partial y}\right)^2 + \left(\frac{\partial u_2}{\partial x}\right)^2 + \left(\frac{\partial u_2}{\partial y}\right)^2\right) - \int_D \left(\frac{\partial u_1}{\partial x}\frac{\partial u_2}{\partial y} - \frac{\partial u_1}{\partial y}\frac{\partial u_2}{\partial x}\right) \\ &= E_D(u) - |\Omega|, \end{aligned}$$

where $E_D(u)$ is the *Dirichlet energy* of u and $|\Omega|$ is the *area* of Ω.

Remark. The above can all be generalised in a straightforward way to the case of arbitrary metrics on D and Ω.

1.2 Numerical Conformal Maps

We now turn to the question of finding a numerical approximation to the unique conformal map $u \in \mathcal{F}_*$. In case D or Ω is a disc, and the standard metric is used in each case, there is an extensive literature involving integral transform techniques, see [Tr]. One usually finds the boundary map directly by these techniques and then extends this map to all of D by finding a numerical approximation to the unique harmonic extension.

A second approach is as follows. It is well known that the unique conformal map in $\mathcal{F}_*$ is characterised by minimising the Dirichlet energy. Let D^h be a triangulation of D of grid "size" h, and suppose that p_1, p_2, p_3 are boundary nodes. Let

$$\begin{aligned}(8)\qquad \mathcal{F}_*^h = \big\{v : D^h \to \Omega \;\big|\, & v \text{ is linear on each face of } D^h,\\ & v\{\text{boundary nodes}\} \subset \partial\Omega,\\ & v \text{ is order preserving on } \{\text{boundary nodes}\},\\ & v(p_i) = q_i \quad \text{for} \quad i = 1, 2, 3\big\}\end{aligned}$$

One can extend v to a map on all of D by first orthogonally projecting $D \setminus D^h$ onto ∂D^h.

It is shown in [T1,2] that if u^h minimises E_D in the class $\mathcal{F}_*^h$, then $u^h \to u$ in $W^{1,2}(D) \cap C^0(\partial D)$, where u is the unique conformal map in $\mathcal{F}_*$. More general results are obtained there in the context of minimal surfaces in R^3. See also [W] and the later discussion in Section 2.

Both these methods have their disadvantages. The integral transform methods only apply in case either D and Ω is a disc, although this can be avoided in principle by a two step process. Moreover, they only apply to the standard metric on D or Ω, although they could presumably be generalised in some cases. Finally, they do not generalise to the case of non-simply connected domains.

The second method is not particularly robust. For example, consider the problem of finding a conformal map from the unit disc to the region bounded by the clover leaf curve

$$g(t) = \big((1 + p\cos 3t)\cos t, (1 + p\cos 3t)\sin t\big). \tag{9}$$

Let p_1, p_2, p_3 on the unit circle and q_1, q_2, q_3 on the clover leaf be given by $t = \pi/3, \pi, 5\pi/3$. Let D^h be the hexagonal triangulation of the unit disc with nl levels where $h = 1/nl$, as shown in Figure 1. In attempting to minimise E_D, u^h will often take a configuration similar to that shown in Figure 2. Thus the Dirichlet energy is minimised by decreasing the area of the image of u^h. See further discussion in the following section.

One can avoid this problem by adding a penalty term corresponding to the area "defect". This is in fact equivalent to the following approach for an appropriate choice of penalty term. However, the simple addition of a penalty term is not natural in the more general situation of minimal surfaces as discussed in Section 2.

1.3 A New Numerical Technique for Finding Conformal Maps

An alternative approach to the previous two methods is to minimise the Conformal Energy directly, rather than the Dirichlet Energy. Clearly $E_C(u) \geq 0$, and $E_C(u) = 0$ iff u is conformal. Thus minimisers of $E_C(u)$ are conformal.

On the other hand we note from (6), c.f.(7), that

$$E_D(u^h) = E_C(u^h) + A(u^h), \tag{10}$$

where $A(u^h) = |\Omega^h|$ is the signed area of the image of D_h. It is clear then from (10) that u^h will attempt to minimise $E_D(u^h)$ by decreasing $|\Omega^h|$. This explains the fact noted before that if one tries to minimise the Dirichlet energy one often observes that the images of the boundary nodes slide around $\partial\Omega$ and the image surface tends to degenerate.

In Figures 2 and 3 we indicate the difference between minimising the Dirichlet energy and minimising the conformal energy in two particular cases for the clover leaf curve.

The conformal energy approach gives much more satisfactory results. The minimisation procedure used is outlined in the following section.

Remark. It is straightforward to extend this approach to the case of arbitrary metrics. In particular one can use the method to find a conformal map from a domain in R^2 to a surface in R^3 with the induced metric.

We note that in case Ω is the unit disc with the standard metric, a related approach is taken in [CA] where the Cauchy Riemann equations are solved directly by a finite difference scheme.

In the next Proposition we justify the approach of minimising conformal energy, making essential use of a result from [T2] where a similar result is established for the Dirichlet energy approach.

Theorem 1. *If $u^h \in \mathcal{F}_*^h$ is the conformal minimiser obtained as above, then $u^h \to u$ in $W^{1,2}(D) \cap C^0(\partial D)$ as $h \to \infty$, where u is conformal.*

Proof. Fix $x_0 \in \Omega$. Then

$$|\Omega^h| = \int_{\partial\Omega^h} (x - x_0) \cdot dt \le d|\partial\Omega^h| \le d|\partial\Omega|,$$

where t is the unit tangent vector to $\partial\Omega^h$ and d is the diameter of Ω. Thus $|\Omega^h|$ is bounded independently of h (this is not immediately obvious because Ω^h may be "multiply covered" by u^h).

It follows from (10) that $E_D(u^h)$ is bounded independently of h. Moreover $\{u^h\}$ is bounded uniformly in L^∞ by the discrete maximum principle. On passing to a subsequence it follows that $u^h \rightharpoonup u$ weakly in $W^{1,2}(D)$ for some $u \in \mathcal{F}_*$. From [T2, Lemma 6] one has moreover that $u^h \to u$ uniformly in $C^0(\partial D)$. It then follows that $|\Omega^h| \to |\Omega|$.

Thus

$$\frac{1}{2}\int_\Omega |Du - Du^h|^2 = -\frac{1}{2}\int_\Omega |Du|^2 + \frac{1}{2}\int_\Omega |Du^h|^2 + \int_\Omega Du(Du - Du^h)$$

$$= -|\Omega| + |\Omega^h| + E_C(u^h) + \int_\Omega Du(Du - Du^h).$$

Hence $\int_\Omega |Du - Du^h|^2 \to 0$, and since $u^h \to u$ uniformly in $C^0(\partial D)$ it follows from the appropriate version of Poincaré's inequality that $u^h \to u$ in $W^{1,2}(D)$.
Moreover

$$\begin{aligned} E_D(u) &\le \liminf E_D(u^h) \\ &= \liminf\big(E_C(u^h) + A(u^h)\big) \\ &= |\Omega|, \end{aligned}$$

since $|\Omega^h| \to |\Omega|$ by the above and $E_C(u^h) \to 0$ by the following proposition.
From (7) it follows that $E_D(u) = |\Omega|$ and u is conformal. Finally, since there is a unique conformal $u \in \mathcal{F}_*$, the original sequence (rather than just a subsequence) converges to u. *Q.E.D.*

The proof of [T2, Lemma 6] uses the Courant-Lebesgue Lemma, and so does not give better than logarithmic type convergence. We hope to address the more subtle question of order h convergence in the $W^{1,2}(D)$ norm in a subsequent paper.

None-the-less, a more natural notion of the failure of u^h to be conformal, rather than $||u - u^h||_{W^{1,2}}$, is $E_C(u - u^h) = E_C(u^h)$, and in this sense one has order h^2 convergence.

Proposition 2. *With notation as before,*

$$E_C(u - u^h) = E_C(u^h) \le ch^2,$$

for some constant c independent of h.

Proof. The equality follows from (5) and the fact that u is conformal. The inequality follows from the fact that if v^h is the piecewise linear approximation to u which agrees with u at the nodes of D^h, then it is straightforward to show that $E_C(v^h) \le ch^2$. *Q.E.D.*

Remark In many applications it is not natural to specify three points p_1, p_2, p_3 and their images q_1, q_2, q_3. Moreover, different choices of normalising points will lead to significant differences in $E_C(u^h)$ for the minimiser $u_h \in \mathcal{F}^h_*$.

Thus let $\mathcal{F}^h$ be defined as in (8), but without the requirement that $v(p_i) = q_i$. While the absolute minimium of $E_C(v)$ in $\mathcal{F}^h$ is taken by the constant maps, in numerical minimisation procedures one will usually obtain a local minimum u^h near some non-trivial conformal map u (assuming one begins the minimisation procedure with some reasonable initial map u_0). This is not surprising in light of the proof of Proposition 2 where it was noted that the piecewise linear approximation to a conformal map u had conformal energy at most ch^2. On the other hand, minimising the Dirichlet energy in $\mathcal{F}^h$ will quite often actually give a constant map. The contrast is usually even more striking than that shown by the examples in Figures 2 and 3, where the images of three points are specified. The difference between the two approaches can again be understood qualitatively by the presence of the area term in (10).

In practice, it is better to begin the conformal minimisation procedure in the class $\mathcal{F}^h$, but when the procedure begins to converge, the rate of convergence can then be improved by fixing the images of three of the boundary nodes.

Alternatively, one can normalise by factoring out motions tangent to the conformal group at the identity, as discussed in Section 2.

1.4 Outline of Numerical Algorithm

Fix $\gamma : S^1 \to \partial\Omega$. For $v \in \mathcal{F}^h_*$ let $\{(x_i^1, x_i^2) \mid i = 1, \ldots, M\}$ and $\{\gamma(t_i) \mid i = 1, \ldots, N\}$ be the images under v of the interior and boundary nodes respectively of D^h.

Thus we define

$$E(x_1^1, \ldots, x_M^1, x_1^2, \ldots, x_M^2, t_1, \ldots, t_N) (= E(x,t)) = E_C(v)$$

We want to minimise E in R^{2M+N}, subject to the constraint

$$t_1 \leq t_2 \leq \ldots t_N \leq t_1 + 2\pi. \tag{11}$$

It is straightforward to compute $E(x,t)$ and grad $E(x,t)$ (note that both these expressions will depend on the map γ), and one can then use various minimisation packages. In practice it is not usually necessary to impose the constraint (11), as it will normally be automatically maintained. We used the LBFGS minimisation package of Nocedal [No], [LN].

2. MINIMAL SURFACES

2.1 General Considerations

Suppose Γ is a C^1 imbedded curve in R^3. Let D be the unit disc in R^2. Then we say u is a *conformally parametrised minimal surface* with boundary Γ if

$$u : D \to R^3,$$

$$u\big|_{\partial D} \text{ is a monotone parametrisation of } \Gamma,$$

$$\Delta u = 0,$$

$$\left|\frac{\partial u}{\partial x}\right| = \left|\frac{\partial u}{\partial y}\right|, \quad u_x \cdot u_y = 0.$$

This is the stationarity condition for the variational problem of minimising $\int_D |Du|^2$ in the class

$$\mathcal{F} = \big\{u : D \to R^3 \bigm| u \in W^{1,2}(D) \cap C^0(\partial D), \quad u|_\Gamma \text{ is a weakly monotone parametrisation of } \Gamma\big\}. \tag{12}$$

Let

$$\mathcal{F}_* = \big\{u \in \mathcal{F} \bigm| u(p_i) = q_i \text{ for } i = 1,2,3\big\}. \tag{13}$$

Let

$$\mathcal{F}^h_* = \{v : D^h \to R^3 \,|v \text{ is linear on each face of } D^h, \tag{14}$$
$$v\{\text{boundary nodes}\} \subset \Gamma,$$
$$v \text{ is order preserving on } \{\text{boundary nodes}\},$$
$$v(p_i) = q_i \quad \text{for} \quad i = 1, 2, 3\}$$

For $u \in \mathcal{F}$ we define the *conformal energy* (analogously to (7)) by

$$\begin{aligned} E_C(u) &= \frac{1}{2}\int_D \left| J(u)\frac{\partial u}{\partial x} - \frac{\partial u}{\partial y}\right|^2 \\ &= \frac{1}{2}\int_D |Du|^2 - \int_D \mathrm{Jac}(u) \\ &= E_D(u) - |u(D)|, \end{aligned} \tag{15}$$

where $J(u)$ is *rotation* through $\pi/2$ in the oriented tangent plane to the image of u (assuming sufficient smoothness of u), $\mathrm{Jac}(u)$ is the *Jacobian* of the map u (i.e. the square root of the sum of the squares of the 2×2 minors of the 2×3 matrix Du), $E_D(u)$ is the *Dirichlet energy* of u, and $|u(D)|$ is the *area* of the *image* of u.

Notice $E_C(u) \geq 0$ and $E_C(u) = 0$ if u is a conformal map. Moreover, u is a conformally parametrised minimal surface iff u is harmonic and $E_C(u) = 0$.

If we attempt to obtain minimal surfaces by minimising $E_D(u)$ in the class $\mathcal{F}^h_*$, we quickly run into the same problem as occurred in the case of conformal maps; that of points sliding around the boundary and the surface "pulling away" from the boundary as in Figure 2. On the other hand it is no longer satisfactory to minimise $E_C(u)$. The problem here is that there is a conformal parametrisation of any smooth surface, and thus no canonical candidate for the conformal energy minimiser in $\mathcal{F}_*$.

In the smooth case one might attempt to proceed as follows. Beginning with some initial map v_0 which minimises the Dirichlet energy subject to its own boundary values, find a conformal u_0 with the *same* image. Let v_1 be the Dirichlet minimiser having the same boundary values as u_0 and find a conformal u_1 with the *same* image as v_1. Proceeding in this way we obtain a sequence $\{u_k\}$ which has monotonely nonincreasing Dirichlet energy. This should converge to a local Dirichlet minimiser. Implementing a version of this in the discrete case is indeed possible, and avoids the problem of the surface pulling away from the boundary, but convergence is very slow and not accurate. See [R] for a related idea.

A much more satisfactory approach is to work in the class of boundary maps; c.f. the Douglas approach and the Morse theory approach to the Plateau problem in [Co] and [St]. Let

$$\mathcal{M} = \Big\{ u : \partial D \to \Gamma \;\Big|\; u \in W^{1,2}(\partial D), u \text{ is a weakly monotone parametrisation of } \Gamma \Big\}. \tag{16}$$

Each $u \in \mathcal{M}$ has a unique harmonic extension to a map $\hat{u}$ defined over D. Write $E_C(u)$ for $E_C(\hat{u})$. Then $E_C(u) \geq 0$ and $E_C(u) = 0$ iff $\hat{u}$ is a conformally parametrised minimal surface. Thus u minimises $E_C(u)$ in $\mathcal{M}$ iff $\hat{u}$ is a minimal surface, and all minimal surfaces are obtained in this way.

Thus minimising $E_C(u)$ in $\mathcal{M}$ has the very significant advantage of giving the *unstable* minimal surfaces as well as the local minimisers.

A natural numerical procedure is to define

$$\begin{aligned} \mathcal{M}^h_* = \Big\{ v : \partial D^h \to R^3 \;\Big|\; & v \text{ is linear on each edge of } \partial D^h, \\ & v\{\text{boundary nodes}\} \subset \Gamma, \\ & v \text{ is order preserving on } \{\text{boundary nodes}\}, \\ & v(p_i) = q_i \quad \text{for} \quad i = 1, 2, 3 \Big\}. \end{aligned} \tag{17}$$

Each $v \in \mathcal{M}^h_*$ has a unique discrete harmonic extension to a map $\hat{v}$ defined over D^h (obtained by minimising the Dirichlet energy in $\mathcal{F}^h_*$ with boundary values v). Write $E_C(v)$

for $E_C(\hat{v})$. If v minimises $E_C(v)$ in $\mathcal{M}_*^h$, then $\hat{v}$ will approximate a (possibly unstable) minimal surface. We discuss convergence questions elsewhere.

2.2 Outline of Numerical Algorithm

Fix a parametrisation $\gamma : S^1 \to \Gamma$. For $v \in \mathcal{M}_*^h$ let $x = \{(x_i^1, x_i^2, x_i^3) \mid i = 1, \ldots, M\}$ and $y = \{(y_i^1, y_i^2, y_i^3) \mid i = 1, \ldots, N\}$ be the images under $\hat{v}$ of the interior and boundary nodes respectively of D^h. Let $t = (t_1, \ldots, t_N)$ be determined by $y_i = \gamma(t_i)$ for $i = 1, \ldots, N$. Note that v and $\hat{v}$ are uniquely determined by t, and conversely.

Next define

$$
\begin{aligned}
(18) \qquad E(t) &:= E_C(v) = E_C(\hat{v}) \\
&= E_D(\hat{v}) - A(\hat{v}) \\
&=: E_D(x_1^1, \ldots, x_M^3, y_1^1, \ldots, y_N^3) \\
&\qquad - A(x_1^1, \ldots, x_M^3, y_1^1, \ldots, y_N^3) \\
&=: E_D\big(x(t), y(t)\big) - A\big(x(t), y(t)\big)
\end{aligned}
$$

The problem is to minimise $E(t)$ in R^N, subject to the constraint

$$
(19) \qquad t_1 \le t_2 \le \ldots t_N \le t_1 + 2\pi .
$$

In order to minimise $E(.)$ we need to be able to compute $E(t)$ and grad $E(t)$ for arbitrary $t \in R^N$.

To compute $E(t)$ first find $\hat{v}$ (by solving the Dirichlet problem) and then compute $E(t) = E_C(v)$.

To compute grad $E(t)$ we proceed as follows.

First note from (18) that

$$\frac{\partial E}{\partial t} = \frac{\partial E_D}{\partial x}\frac{\partial x}{\partial t} + \frac{\partial E_D}{\partial y}\frac{\partial y}{\partial t} - \frac{\partial A}{\partial x}\frac{\partial x}{\partial t} - \frac{\partial A}{\partial y}\frac{\partial y}{\partial t} \tag{20}$$
$$= \frac{\partial E_D}{\partial y}\frac{\partial y}{\partial t} - \frac{\partial A}{\partial x}\frac{\partial x}{\partial t} - \frac{\partial A}{\partial y}\frac{\partial y}{\partial t},$$

since $\partial E_D/\partial x = 0$ from the Dirichlet minimising properties of $\hat{v}$.

The quantities $\partial E_D/\partial y$, $\partial A/\partial x$, $\partial A/\partial y$ and $\partial y/\partial t$ can all be readily computed (the last equals $\gamma'(t)$). We find $\partial x/\partial t$ by differentiating $\partial E_D/\partial x = 0$ with respect to t to obtain

$$\frac{\partial^2 E_D}{\partial x \partial x}\frac{\partial x}{\partial t} = -\frac{\partial^2 E_D}{\partial x \partial y}\frac{\partial y}{\partial t}. \tag{21}$$

Since $\partial^2 E_D/\partial x\partial x$ is positive definite and $\partial^2 E_D/\partial x\partial y$ and $\partial y/\partial t$ are computable, one can solve for $\partial x/\partial t$.

(The computational requirements for solving (21) can be shortened considerably as follows. Note that E_D is quadratic in x and y and so the matrices $\partial^2 E_D/\partial x\partial x$ and $\partial^2 E_D/\partial x\partial y$ are independent of t. Let e_α range over the $3N$ basis vectors for R^{3N} and let z_α be given by

$$\frac{\partial^2 E_D}{\partial x \partial x} z_\alpha = -\frac{\partial^2 E_D}{\partial x \partial y} e_\alpha. \tag{22}$$

The z_α are independent of t and can be computed and stored at the beginning of the minimisation procedure (further simplifications can be achieved by using the symmetries of E_D).

The solutions to (21) are then given by

$$\frac{\partial x}{\partial t_\alpha} = \sum_\beta \frac{\partial y_\beta}{\partial t_\alpha} z_\beta. \tag{23}$$

For each α there are only three non-zero terms in the above sum.)

The minimisation procedure is now clear. Begin with some initial t^0 and use a minimisation package to compute t^{i+1} from t^i, $E(t^i)$, grad $E(t^i)$ and perhaps information from earlier steps. We used the LBFGS procedure of Nocedal [No], [LN]. The (discrete) minimal surface is the solution of the (discrete) Dirichlet problem corresponding to the terminating value of t^i.

In practice the condition (19) is stronger than necessary. One can begin with t^0 subject only to the requirement that it induces a map of S^1 to S^1 with winding number one. The condition (19) will then hold for all t^i with i sufficiently large. See [Ni, Sect 307] and [Co, pp 213-218] for some theoretical justification of this fact.

Instead of normalising by fixing the image of three boundary nodes, we normalised by staying in the class orthogonal to the tangent space at the identity map to the conformal group of the disc, see [St, p 46]. In the smooth case, this is equivalent to restricting to maps of the form $u = \gamma \circ g$ where $g : S^1 \to S^1$ and

$$\int_0^{2\pi} g = \int_0^{2\pi} \theta = 2\pi \qquad \int_0^{2\pi} g\cos\theta = \int_0^{2\pi} g\sin\theta = 0. \tag{24}$$

Equivalently, the Fourier expansion of g is of the form

$$g(\theta) = \theta + \sum_{n=2}^{\infty} \big(a_n \cos n\theta + b_n \sin n\theta\big). \tag{25}$$

2.3 Examples

The curve Γ_r is given by $\gamma(\theta) = \gamma_r(\theta) = (x_r(\theta), y_r(\theta), z_r(\theta))$ where

$$\begin{aligned} x_r(\theta) &= r\cos\theta - \frac{1}{3}r^3\cos 3\theta, \\ y_r(\theta) &= -r\sin\theta - \frac{1}{3}r^3\sin 3\theta, \\ y_r(\theta) &= r^2\cos 2\theta, \end{aligned} \tag{26}$$

for $0 \le \theta \le 2\pi$. If $1 < r < \sqrt{3}$, then Γ_r bounds at least 3 minimal surfaces, of which two are area minimising and one (known as Enneper's surface) is unstable. An explicit conformal representation is given for the latter by the Wieirstrass representation [Ni, Sect.88].

As a test case we took $r = 1.1$ and began with boundary data corresponding to the function g in (25) given by various values of a_n and b_n. The method converged to Enneper's surface with an error of approximately 3 decimal places in the L_2 norm for 16 levels in the triangulation of the unit disc. See Figure 4 for an approximation to Enneper's surface obtained by the present method.

In Figure 5 we show (a discrete approximation to) the absolute minimiser obtained by minimising the Dirichlet energy. For larger values of r this method is not satisfactory due to the "pulling away" phenomenon discussed earlier.

For the initial data considered, the final surface was always Enneper's surface rather than one of the absolute minimisers. We can understand this as follows. The conformal factor of the parametrising map $\hat{u}_1$ for the absolute minimiser takes a much larger range of values than in the case of $\hat{u}_2$ for Enneper's surface (as we see from Figure's 4 and 5). If $\hat{u}_1^h$ and $\hat{u}_2^h$ are the corresponding discrete maps, then it follows that $E_C(u_1^h) >> E_C(u_2^h) > 0$ due to discretisation error. Since the minimisation package tends to find absolute rather than local minima, the method converged to $\hat{u}_2^h$ rather than $\hat{u}_1^h$.

However, for other boundary curves we have found more than one one stationary point for the area (or equivalently, Dirichlet) functional.

In Figure 6 we show a branched minimal immersion. The absolute minimiser has no branch points, as is well known by a cut-and-paste argument. The minimal surface shown is probably unstable, as is indicated by taking it as initial data and minimising the Dirichlet energy. The surface slowly (at first) evolves to an imbedded surface, which eventually "pulls away" from the boundary as discussed earlier (due to the large variation in the conformal factor over the surface).

2.4 Extensions

We are currently implementing a selective refinement algorithm which will significantly decrease the discretisation error. We are also implementing another minimisation procedure which should not favour global over local minima.

Finally we remark that these methods are capable of significant extensions to related problems. We have implemented a preliminary version to obtain minimal surfaces where one part of the boundary is taken on a given one dimensional curve, and the remaining part of the boundary is normal to a two dimensional surface but otherwise free. The method can clearly be generalised to obtain unstable *small* H-surfaces, c.f. [St]. We anticipate that with some further extensions to first obtain unstable solutions to the corresponding Dirichlet problem, the method will be able to also compute unstable *large* H-surfaces.

REFERENCES

[CA] Chakravarthy S. and Anderson D.: Numerical Conformal Mapping, *Math of Comp.*, **33** (1979), 953-969.

[Co] Courant R.: *Dirichlet's Principle, Conformal Energy, and Minimal Surfaces*, Interscience, New York, 1950.

[LN] Liu D.C. and Nocedal J.: On the Limited Memory BFGS Method for Large Scale Optimization, *Math Prog.*, **45** (1989), 503-528.

[Ni] Nitsche J.C.C.: *Lectures on Minimal Surfaces, Volume 1*, Cambridge University Press, 1989.

[No] Nocedal J.: Limited Memory BFGS Method for Large Scale Optimization, *Harwell Software Library*.

[R] Radó T.: An Iterative Process in the Problem of Plateau, *Trans. Amer. Math. Soc.*, **35** (1933), 869-87.

[St] Struwe M.: *Plateau's Problem and the Calculus of Variations*, Mathematical Notes 35, Princeton University Press, Princeton, 1988.

[T1] Tsuchiya T.: Discrete Solution of the Plateau Problem and Its Convergence, *Math. of Comp.*, **49** (1987), 157-165.

[T2] Tsuchiya T.: A Note on Discrete Solutions of the Plateau Problem, *Math. of Comp.*, **54** (1990), 131-138.

[Tr] Trefethen L. N.: *J. Comp. and Appl. Math.*, **14** (1965), entire issue, 15 papers edited by Trefethen.

[W] Wilson W.L.: On Discrete Dirichlet and Plateau Problems, *Num. Math.*, **3** (1961), 359-373.

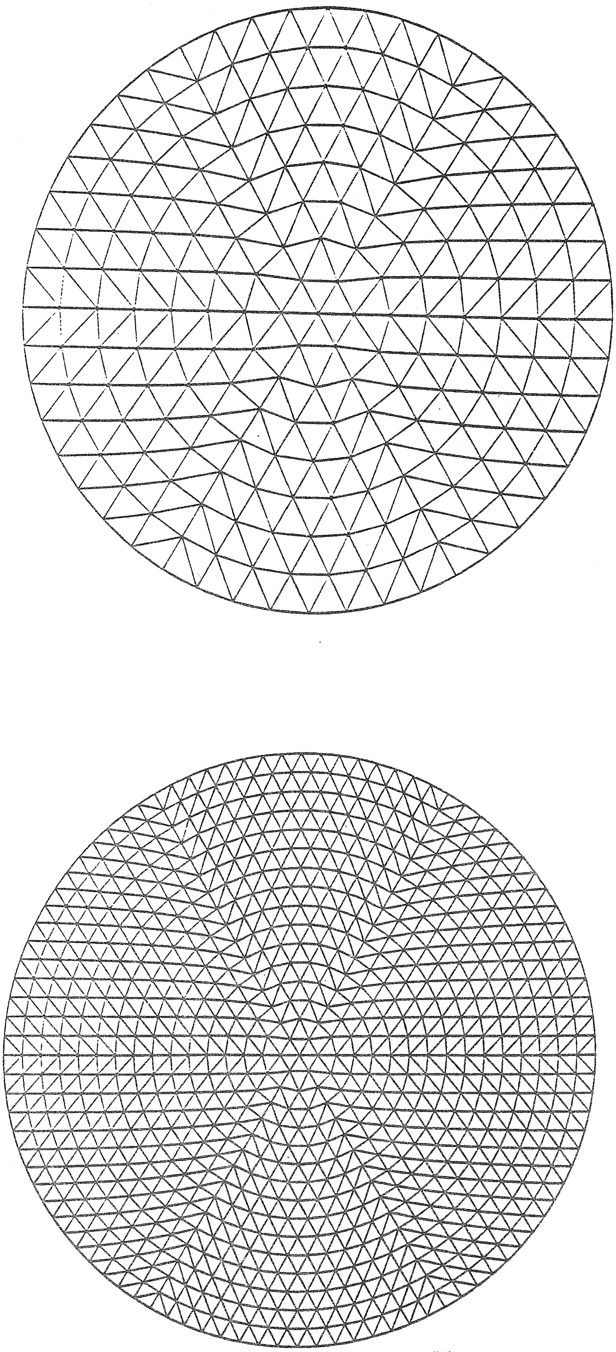

Triangulation of Disc with number of levels nl equal to 8, 16.

Figure 1

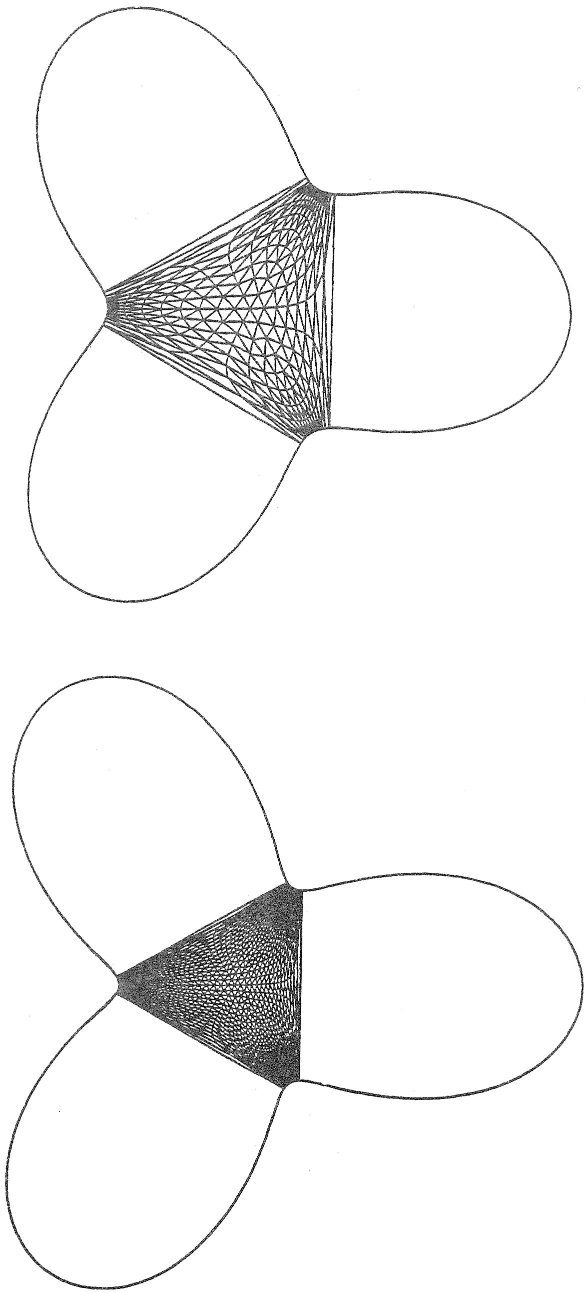

Result of minimising the Dirichlet energy among discrete maps to the clover leaf domain with triangulations corresponding to Figure 1.

Figure 2

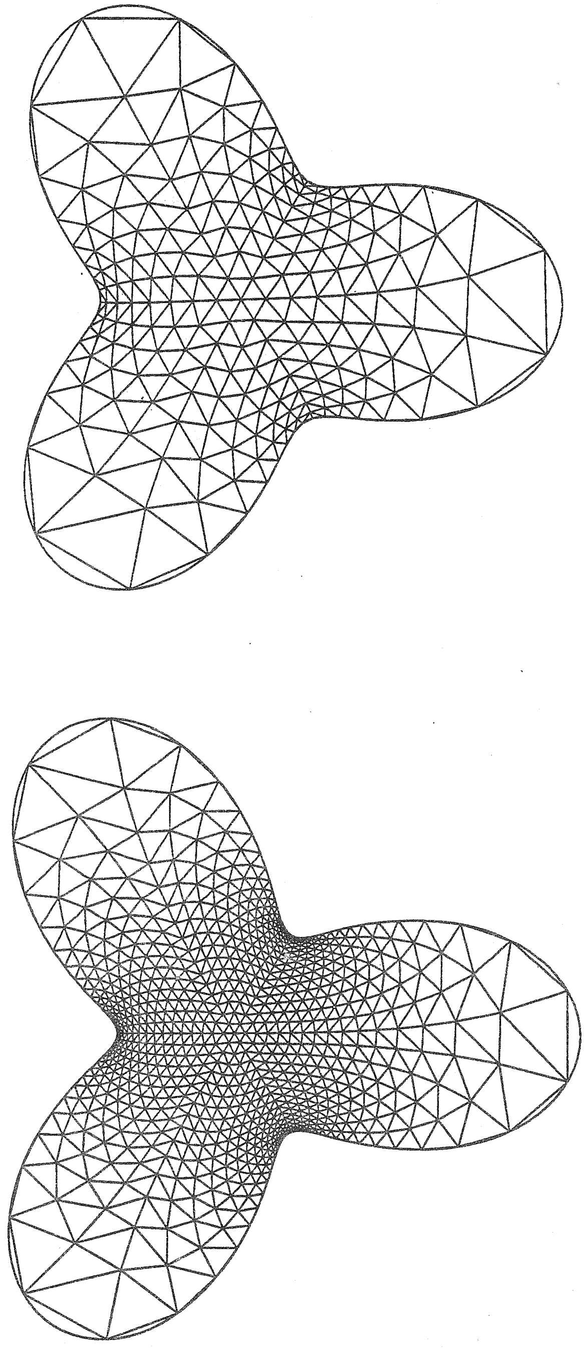

Result of minimising the conformal energy among discrete maps to the clover leaf domain with triangulations corresponding to Figure 1.

Figure 3

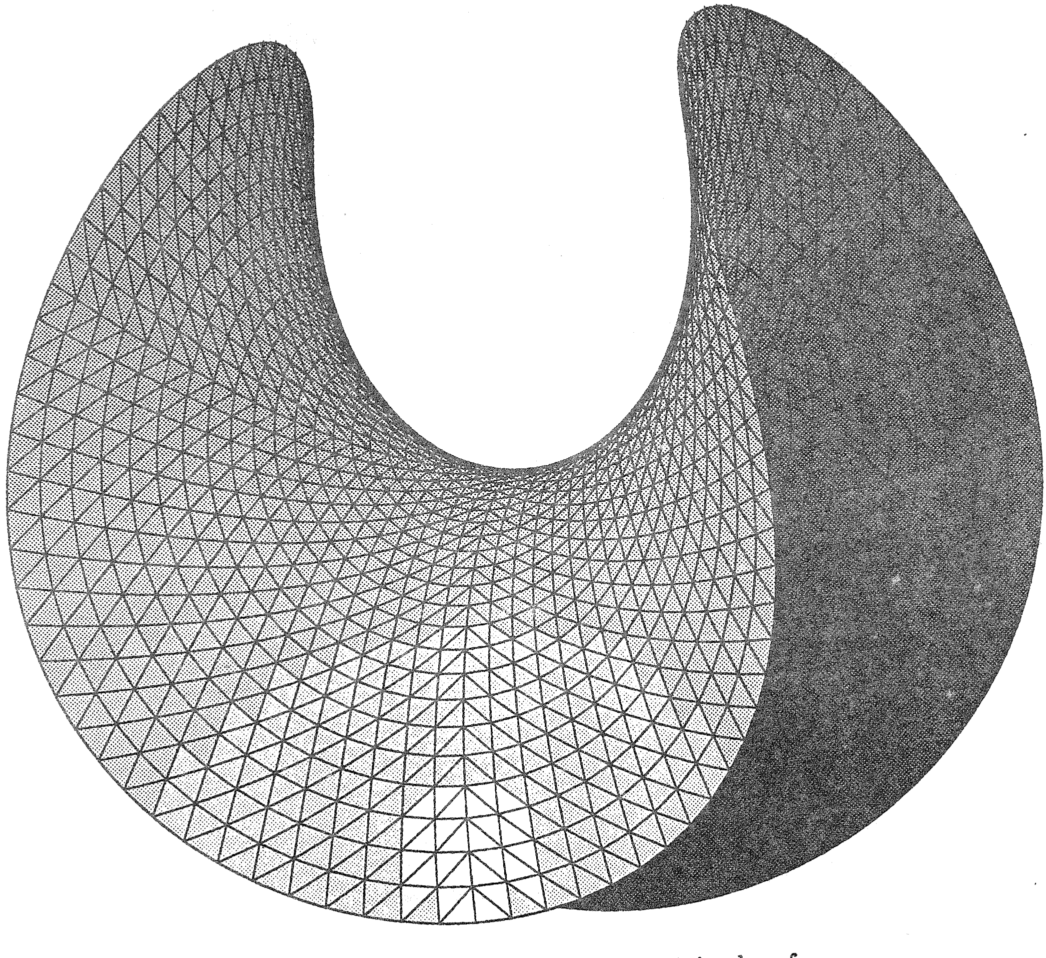

Enneper's surface, an unstable minimal surface.

Figure 4

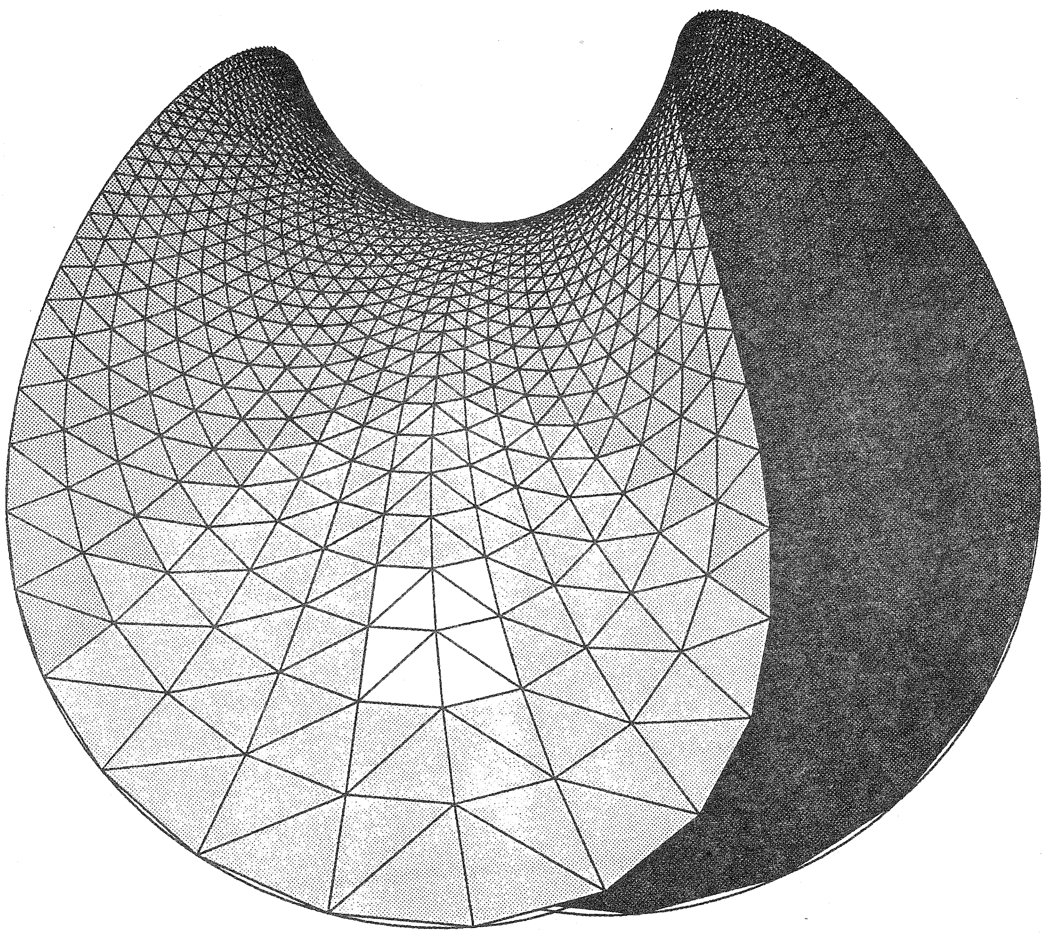

Area minimising surface with the same boundary as Enneper's surface.

Figure 5

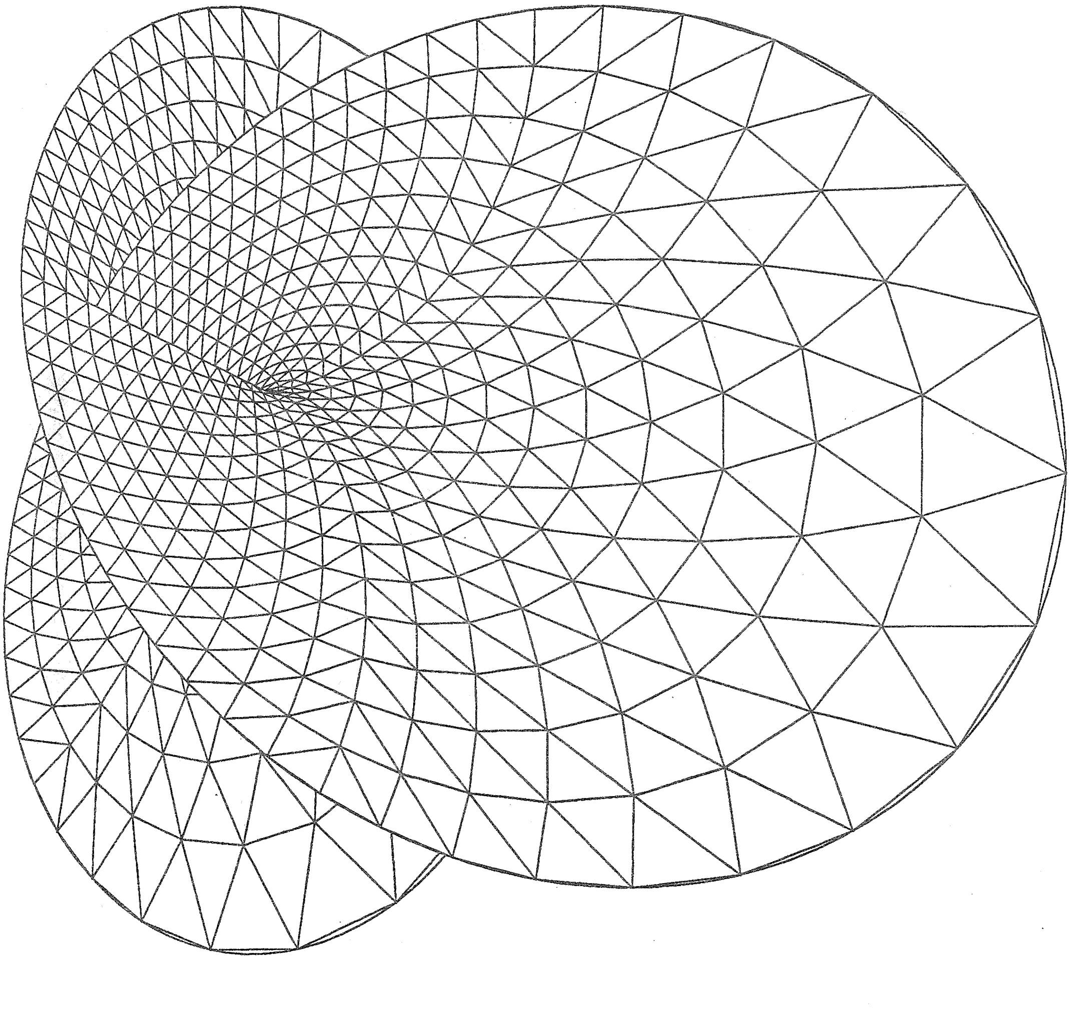

A branched minimal immersion.

Figure 6